DOI 10.31489/2022No1/5-9

UDC 538.9

TEMPERATURE DEPENDENCES OF THE INITIAL PERMEABILITY OF LITHIUM-TITANIUM FERRITES PRODUCED BY SOLID-STATE SINTERING IN THERMAL AND RADIATION-THERMAL MODES

Surzhikov A.P.[1], Malyshev A.V.[1], Lysenko E.N.[1], Stary O.[2]

[1]Tomsk Polytechnic University, Tomsk, Russia, malyshev@tpu.ru
[2]Ceské vysokéucenítechnické v Prague, Prague, Czech Republic

The paper investigates the features of phase and structural transformations in lithium-titanium ferrites with regard to the time and temperature of solid-state sintering in thermal and radiation-thermal modes. These properties are studied with using the temperature dependence of the initial permeability. It is shown that electron beam exposure during solid-state sintering sharply accelerates the dissolution of impurity inclusions in ferrites. Also phase homogeneity of lithium-titanium ferrites products increase. The obtained results can be used for increasing of the phase homogeneity in ferrite production.

Keywords: lithium ferrites, solid-state sintering, electron beams, high temperatures, initial permeability.

Introduction

Electromagnetic properties are the key requirements imposed on ferrite materials during their production and operation. It is known that these properties depend on chemical composition of the mixture and the ferrite manufacturing technique. The main manufacturing operation that largely determines electromagnetic properties of the ferrite material is extremely time-consuming sintering of compacted products. Two-stage introduction of components, additional mixing of ferrite with ferrite powder of similar composition, liquid phase, forced sintering, and ultrasonic assisted sintering are the techniques used to activate sintering [1–10]. These sintering modes increase the occurrence of impurity phases, which decrease chemical and structural homogeneity of the material and deteriorate its electromagnetic properties.

In addition, the impurity phase concentration cannot always be decreased by temperature regime of sintering, especially in case of thermally unstable compounds such as lithium ferrispinels. In recent years, the effect of ionizing radiation fluxes has gained momentum in manufacturing and modification of materials. A fundamental phenomenon of a multiple increase in the speed of multicomponent powder synthesis [11–14] and sintering of compacts [15–19] induced by radiation-thermal mode was discovered. Sintering of lithium-titanium ferrites under specific conditions of a combined effect of high temperatures and intense electron fluxesis the most well studied process [20–22]. The patterns of ferrite compaction were revealed, and a multiple increase in the compaction rate of lithium-titanium ferrites under these sintering conditions was shown [23–25]. Magnetic properties of ferrimagnets are the key functional properties. It is known that any ferrite manufacturing technique is ultimately aimed at achieving the designed performance level. The root causes and features of the formation of ferrite magnetic properties are of particular interest. Therefore, data on phase transformations in ferrites during radiation-thermal (RT) sintering can be important and productive. The paper investigates the features of phase transformations of ferrite ceramics sintered in RT mode using the temperature dependence of the initial permeability. A comparative study of ferrite samples sintered in thermal (T) mode was performed to reveal the radiation effect. XRD analysis cannot be implemented for lithium ferrites due to overlapping of the main lines of the $LiFe_5O_8$, $LiFeO_2$, and Fe_3O_4 phases.

1. Experimental part

1.1 Materials

The study investigates lithium-titanium ferrite powders synthesized from a mechanical mixture of oxides and carbonates containing 11.2 wt% Li_2CO_3, 18.65 wt% TiO_2, 7.6wt% ZnO, and 2.74 wt% $MnCO_3$, and the rest of the mixture is Fe_2O_3. For pressing, 10% solution of polyvinyl alcohol is added in an amount of

12 wt% of the mixture. Compacts are made in the form of annular cores 2 mm thick, with an inner and outer diameter of 18 mm and 14 mm, respectively, by single-action cold pressing using a PGr-10 press.

1.2 Characterization techniques

The optimal compacting pressure is chosen experimentally. It is found that the compacting pressure in the range of (110–200) MPa is optimal to provide an acceptable density of both green and sintered samples. The pressing mode employed was as follows: P=130 MPa;1 min pressing time; RT and T modes of compact sintering. In RT sintering, the compacts were exposed to a pulsed electron beam with energy of (1.5–2.0) MeV generated by the ILU-6 accelerator. The pulse beam current was (0.5–0.9) A, the irradiation pulse duration was 500 μs, the pulse repetition rate was (5–50) Hz, and the compact heating rate was 1000 C/min. The samples were irradiated in a lightweight chamotte box with a wall bottom 15 mm thick. The exposed side of the box was covered with a radiation-transparent cover with a mass thickness of 0.1 $g \cdot cm^{-1}$. Temperature was measured using a control sample placed in close proximity to the sintered compacts.

T sintering was performed in a preheated chamber electric furnace, which provided a heating rate comparable to radiation heating rate. The cell design and temperature control technique are similar to those used for RT sintering. Sintering in both modes was performed in air. Methods for measuring initial permeability (μ_i) available in literature were analyzed, and the method chosen was based on measurement of the ring core inductance in an alternating magnetic field [26].

Measurements were performed for samples sintered in different modes with a single-layer winding uniformly distributed around the core perimeter during sample cooling from the temperature point that intentionally exceeded the Curie point (about 620 K) using an E7-12 inductance meter at 1 MHz frequency. Temperature dependence of μ_i was determined from temperature dependence of inductance by formula 1:

$$\mu_i = L/L_0\,, \tag{1}$$

where L and L_o are winding inductance with and without a ferrite core.

The minimum value of the inductance L at temperature above the Curie point was taken for inductance of the winding without a core L_o. The validity of using L_o as winding inductance is confirmed by direct calculation performed for toroidal rectangular cores by formula 2:

$$L_0 = 2 \cdot 10^{-3} \cdot N^2 \cdot h \cdot \ln(D_2/D_1) \text{ (μH/cm)}, \tag{2}$$

where N is the number of turns; h is sample thickness; D_1 and D_2 are the inner and outer diameter of the core.

2. Results and discussion

Fig. 1 shows the curves of initial permeability μ_i against temperature for ferrites sintered at 1373 K in T and RT modes. All curves in Fig. 1 demonstrate an increase in initial permeability at increased temperature with its maximum achieved near the Curie point.

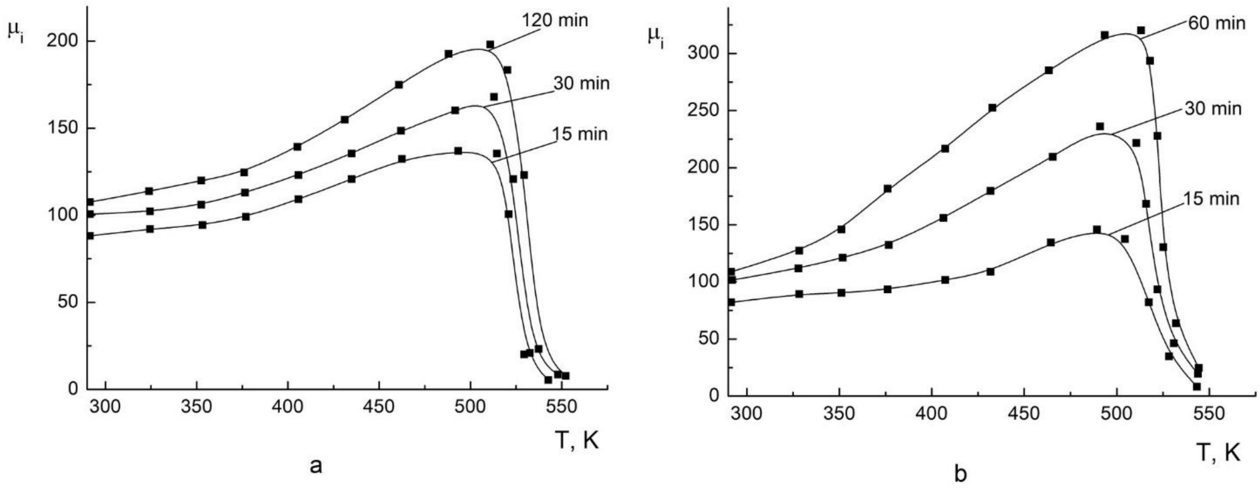

Fig.1. Temperature dependence of μ_i for ferrites sintered at 1373 K in T (a) and RT (b) modes for different sintering time

After the maximum, permeability steeply declines and remains stable beyond the Curie point. The μ_i value at the temperature dependence maximum ($\mu_{i\ max}$) grow as sintering time increases, and the rate of its growth in RT mode significantly exceeds the growth rate of $\mu_{i\ max}$ in T mode. The kinetic dependences of initial permeability are shown in Fig. 2.

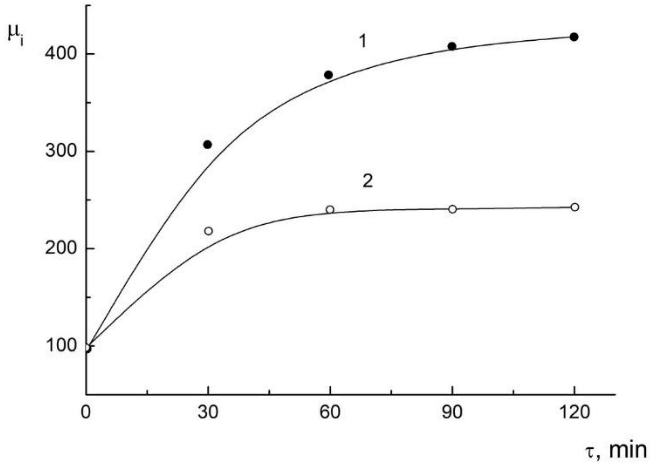

Fig.2. Dependence of $\mu_{i\ max}$ on time of ferrite sintering at 1373 K in T (1) and RT (2) modes

The data in Fig. 2 show a more complete inclusion removal for RT mode. The difference in sample density (1 h sintering time) was ~5%, and the difference in $\mu_{i\ max}$ was ~32% in both sintering modes, therefore it can be assumed that inclusion removal is not due to porosity removal, but due to probable dissolution of impurity phases in the main product. The features of the temperature drop $\mu_i(T)$ were analyzed based on the graphs of the rate of decrease in permeability $d\mu_i/dT$ against temperature plotted in Fig. 3.

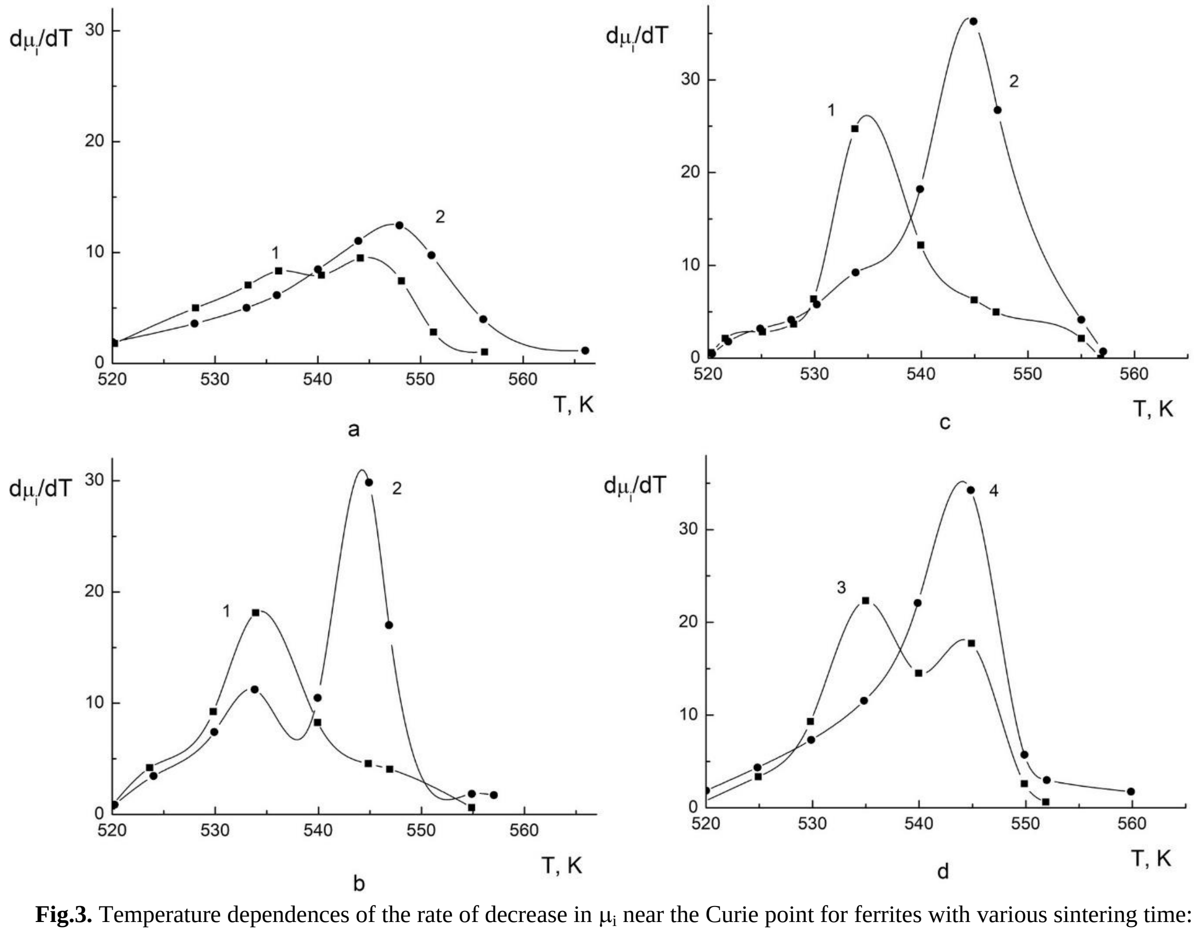

Fig.3. Temperature dependences of the rate of decrease in μ_i near the Curie point for ferrites with various sintering time: *a*) 15 min; *b*) 30 min; *c*) 60 min; *d*) 300 min (3) and 600 min (4). *1, 3, 4* – T sintering mode, 2 – RT sintering mode

As can be seen, these dependences exhibit two distinct and consistently repeated peaks at 537 and 548 K. This indicates at least two chemically similar magnetic phases in the sample. Typically, a low-temperature phase predominates at early (up to 2 h) sintering stages in T mode (Fig. 3, *a*, *b*, *c*). Sintering for 5 h equalizes the content of both phases (Fig. 3*d*, curve *3*), and after10 h sintering, a high-temperature phase dominates (Fig. 3*d*, curve *4*) [27, 28].

RT sintering yields a qualitatively different result a high-temperature phase dominates at all sintering stages, although traces of the low-temperature phase were detected as well (Fig. 3, *a*, *b*, *c*). No correlation is found for the change in the content of both phases, which can imply that a high-temperature magnetic phase is formed mainly due to non-magnetic inclusions [29, 30].

Conclusion

In this article, from a comparative study of temperature dependencies of initial permeability lithium ferrites at radiation-thermal and thermal solid-phase sintering, the share of the radiation component in the formation of electromagnetic parameters of the material is established.

The scientific significance of the results is determined by data on the temperature dependences of the initial permeability shows that electron beam exposure during sintering of lithium-titanium ferrite compacts sharply accelerates dissolution of impurity inclusions.

The possibility of using an electron beam to increase phase homogeneity of ferrite products during their manufacturing makes the study results practically relevant.

The next step is to study the same patterns in liquid-phase ferrite sintering under the same radiation-thermal and thermal conditions. In addition, the share of the radiation component in such sintering will be determined and the results of this article will be compared with subsequent studies. Also, the effects will be determined depending on the type of sintering.

Acknowledgments

The research is funded by the Ministry of Education and Science of the Russian Federation as part of the "Science" Program (project No. FSWW-2020-0014). This research was supported by TPU development program.

REFERENCES

1 Letyuk L.M., Nifontov V.A., Babich E.A., Gorelik S.S. Effect of low-melting additives on the formation of the microstructure and the properties of ferrites with a rectangular hysteresis loop. *Izv. Akad. Nauk Neorg. Mater*. 1976, Vol. 12, pp. 2023 – 2026. [in Russian]

2 Dmitriev M.V., Letyuk L.M., Shipko M.N. Study of oxygen diffusion in the surface layers of Mn-Zn ferrites. *Technical physics*. 1982, Vol. 27, pp. 338 – 339.

3 Letyuk L.M. Recrystallization of ferrites and its effect on the processes of microstructure formation in ferrospinels. *Soviet Powder Metallurgy and Metal Ceramics*. 1980, Vol. 19, No. 5, pp. 359 – 364.

4 Zinovik M.A., Zinovik E.V. Ferrites with rectangular and square hysteresis loops. *Powder Metallurgy and Metal Ceramics*. 2005, Vol. 44, pp. 66 – 74.

5 Letyuk L.M., et al. Special features of the formation of the microstructure of ferrites sintered in the presence of a liquid phase. *Izv.Vysshikh Uchebnykh Zavedenij. Chernaya Metallurgiya*. 1979, Vol. 11, pp. 124 – 127. [in Russian]

6 Micheli A.L. Preparation of lithium ferrites by coprecipitation. *IEEE Transactions on Magnetics*. 1970, Vol. 6, pp. 606 – 608.

7 Surzhikov A.P., Pritulov A.M., Lysenko E.N., et al. Calorimetric investigation of radiation-thermal synthesized lithium pentaferrite. *J. Therm. Anal. Calorim.* 2010, Vol. 101, No. 1, pp. 11 – 13.

8 Minin V.M. Effect of sintering conditions on the microstructure and electromagnetic properties of Li-Mg-Mn ferrite memory elements. *Soviet Powder Metallurgy and Metal Ceramics*. 1982, Vol. 21, pp. 698 – 701.

9 Zahir R., Chowdhury F.-U.-Z., Uddin M.M., et al. Structural, magnetic and electrical characterization of Cd substituted Mg ferrites synthesized by double sintering technique. *J. Magn. Magn. Mater*. 2016, Vol. 410, pp. 55 – 62.

10 Manjura Hoque S., Abdul Hakim M., Mamun Al, et al. Study of the bulk magnetic and electrical properties of $MgFe_2O_4$ synthesized by chemical method. *Materials Sciences and Applications*. 2011, Vol. 2, pp. 1564 – 1569.

11 Surzhikov A.P., Pritulov A.M., Lysenko E.N., et al. Influence of solid-phase ferritization method on phase composition of lithium-zinc ferrites with various concentration of zinc. *Journal of Thermal Analysis and Calorimetry.* 2012, Vol. 109, No. 1, pp. 63 – 67.

12 Yurov V.M., Baltabekov A.S., Laurinas V.C., Guchenko S.A. Dimensional effects and surface energy of ferroelectric crystals. *Eurasian Physical Technical Journal*. 2019, Vol. 16, No. 1, pp. 18 – 23.

13 Lyakhov N.Z., Boldyrev V.V., Voronin A.P., Gribkov O.S., Bochkarev I.G., Rusakov S.V., Auslender V.L. Electron beam stimulated chemical reaction in solids. *J. Therm. Anal. Calorim*. 1995, Vol. 43, pp. 21 – 31.

14 Sharma P., Uniyal P. Investigating thermal and kinetic parameters of lithium titanate formation by solid-state method. *J. Therm. Anal.Calorim*. 2017, Vol. 128, pp. 875 – 882.

15 Salimov R.A., Cherepkov V.G., Golubenko J.I., et al. D.C. high power electron accelerators of ELV-series: status, development, applications. *J. Radiation Phys. Chem*. 2000, Vol. 57, pp. 661 – 665.

16 Cleland M.R., Parks L.A. Medium and high-energy electron beam radiation processing equipment for commercial applications. *Nucl. Instr. Meth. B.* 2003, Vol. 208, pp. 74 – 89.

17 Mehnert R. Review of industrial applications of electron accelerators. *Nucl. Instr. Meth.B.* 1996, Vol. 113, pp.81 – 87.

18 Neronov V.A., Voronin A.P., Tatarintseva M.I., Melekhova T.E., Auslender V.L. Sintering under a high-power electron beam. *J. Less-Common Metals*. 1986, Vol. 117, pp. 391 – 394.

19 Ershov B.G. Radiation technologies: their possibilities, state, and prospects of application. *Herald of the Russian Academy of Sciences*. 2013, Vol. 83, No. 5, pp. 437 – 447.

20 Surzhikov A.P., Frangulyan T.S., Ghyngazov S.A. A thermoanalysis of phase transformations and linear shrinkage kinetics of ceramics made from ultrafine plasmo-chemical ZrO_2(Y)-Al_2O_3 powders. *Journal of Thermal Analysis and Calorimetry*. 2014, Vo. 115, № 2, pp. 1439 – 1445.

21 Stary O., Malyshev A.V., Lysenko E.N., Petrova A. Formation of magnetic properties of ferrites during radiation-thermal sintering. *Eurasian phys. tech. j.* 2020, Vol. 17, No. 2, pp. 6 – 10.

22 Boldyrev V.V., Voronin A.P., Gribkov O.S., Tkachenko E.V., Karagedov G.R., Yakobson B.I., Auslender V.L. Radiation-thermal synthesis. Current achievement and outlook. *J. Solid State Ion.* 1989, Vol. 36, pp. 1 – 6.

23 Surzhikov A.P., Frangulyan T.S., Ghyngazov S.A., Vasil'ev I.P., Chernyavskii A.V. Sintering of zirconia ceramics by intense high-energy electron beam. *Ceramics Int.* 2016, Vol. 42, No. 12, pp. 13888 – 13892.

24 Nikolaev E.V., Astafyev A.L., Nikolaeva S.A., et al. Investigation of electrical properties homogeneity of Li-Ti-Zn ferrite ceramics. *Eurasian phys. tech. j.* 2020, Vol. 17, No. 1, pp. 5 – 12.

25 Sharipov M.Z., Hayitov D.E., Rizoqulov M.N., Islomov U.N., Raupova I.B. Domain structure and magnetic properties of terbium ferrite-garnet in the vicinity of the magnetic compensation point. *Eurasian Physical Technical Journal*. 2019, Vol. 16, No. 2(32). pp. 21 – 25.

26 Smith J., Wijn H.P.J. *Ferrites: Physical properties of ferromagnetic oxides in relation to their technical application.* 1959, Eindhoven, Phillips Technical Library, 233p.

27 Neronov V.A., Voronin A.P., Tatarintseva M.I., et al. Sintering under a high-power electron beam. *Journal of the Less Common Metals*. 1986, Vol. 117, pp. 391 – 394.

28 Geguzin J.E. *Physics of Sintering*. 1984, Moscow, Nauka, 360p. [in Russian]

29 Takane S., Umeda H., Aoki T., Murase T. Influence of Al_2O_3 Addition on the temperature dependence of initial permeability of NiCuZn ferrites. *Key Eng. Mater.* 2011, Vol. 485, pp. 225 – 228.

30 Malyshev A.V., Petrova A.B., Surzhikov A.P., Sokolovskiy A.N. Effect of sintering regimes on the microstructure and magnetic properties of LiTiZn ferrite ceramic. *Ceramics Int.* 2019, Vol. 45, pp. 2719 – 2724.

Article accepted for publication 09.09.2021